Characterization of kaolinite aqueous suspensions by acoustophoresis: Influence of crystallinity and of the ratio between basal and lateral surface of grains

Rana Al-Tahan, Richard Mayet, Patrice Duport, Nicolas Tessier-Doyen, Anne Aimable, Gilles Gasgnier, Cécile Pagnoux

Version of Record: https://www.sciencedirect.com/science/article/pii/S0927775722012286
Manuscript_c7916a24bcd1a1de7a363ff79ae4fa54

Characterization of kaolinite aqueous suspensions by acoustophoresis: influence of crystallinity and of the ratio between basal and lateral surface of grains.

Rana Al-Tahan[1], Richard Mayet[1], Patrice Duport[1], Nicolas Tessier-Doyen[1], Anne Aimable[1], Gilles Gasgnier[2], Cécile Pagnoux[1]

[1.] IRCER, Centre Européen de la Céramique, Université de Limoges, 12 rue Atlantis, 87068 Limoges, France

[2.] Imerys Tableware France, 1 rue Jeanne d'Albret, 87700 Aixe-sur-Vienne

Abstract

The electrokinetic properties of aqueous suspensions of two kaolins were studied using the acoustophoretic method by measuring the ultrasonic attenuation spectrum in a wide frequency range (1-20 MHz). Then, the zeta potential is calculated according to the size distribution of grains. A high state of crystallinity of the kaolinite platelets strongly influences the amplitude and the variation of zeta potential versus the pH due to a high density of hydroxyl surface groups. It was also shown that ion exchanges occur mainly with the hydroxyl surface groups of the platelet edges by using strong electrolytes (NaOH and HCl) but also organic molecules (Tiron and sodium salt of citrate) specifically adsorbed. The variation of the surface chemistry properties of platelets during the amorphous phase formation after temperature treatment of kaolin powder is also studied. The electrokinetic properties of kaolin suspensions treated between 200 and 800 °C successively show an increase in the positive contribution to the zeta potential up to 400 °C for the best-crystallized kaolinite and a decrease in the density of surface hydroxyl groups when the sheets delaminate from 400 °C for the less-crystallized kaolinite. This study shows that the characterization in aqueous suspension of surface properties of kaolinite complements other studies carried out on powder and therefore it makes it possible to choose kaolin as a raw material according to the intended application.

Keywords

Kaolinite, Surface charge modifications, Acoustophoresis, Thermal behaviour, Tiron, Citrate.

1. Introduction

Kaolinite is one of the most studied mineral precursors because of its interesting characteristics. A great thermal resistance, a high melting point, and electrical non-conductivity make it commonly used in ceramic manufacturing (porcelain, bricks, potteries, and tiles). Furthermore, its natural whiteness, chemical stability, fine particle size, and high readily dispersion in water and some organic systems are used to produce suspensions combining a low viscosity with a proportion of solid phase in many systems. It also has a wide variety of applications including as an adsorbent for the removal of heavy metals and dyes including Pb^{2+}, Ni^{2+} and Cu^{2+} from aqueous solutions, as a chemical component in cement manufacturing, food additives, cosmetics, as a filler in the manufacture of fiberglass and paper industry, etc [1]–[8].

However, the physicochemical characteristics of kaolinite, including the crystal order, specific surface area, morphology, and surface properties vary depending on the source of kaolin [9]. Each kaolin powder is specific depending on the deposit, which has its own chemical composition, substitution in the sheets, grain shape, etc.

Kaolinite ($Al_2Si_2O_5(OH)_4$) is a 1:1 dioctahedral phyllosilicate, the main mineral of kaolins. The ideal composition is Al_2O_3 39.53%, SiO_2 46.51%, and H_2O 13.96%. It generally crystallizes in the form of pseudo-hexagonal platelets with a small thickness (from 1 µm to 100 nm). The shape of these grains, composed of stacks of several sheets associated with a structural anisotropy, promotes complex surface properties with faces/edges of alumina (layers of octahedrons $AlO_2(OH)_4$) or silica (layers of tetrahedrons SiO_4) types. The hydroxyl groups in kaolinite exist in two forms connected to Al in the aluminium sheet, inner-surface hydroxyl groups on the inner surface of the sheet

opposite the tetrahedral oxygen on the one hand, and on broken edges and upper surface of kaolinite called outer hydroxyl groups on the other hand.

In aqueous media, the kaolinite has a heterogeneous surface charge which can be described by a patch-wise model of kaolinite platelets [10]. It is based on the dissociation of the surface charge contributions attributed to the basal and lateral surfaces of the platelets. Edges are generated as a result of broken bonds and are composed of alternating alumina and silica sites. The electrical charges developed onto the surface of the grains of kaolinite and their dispersion are affected by several parameters including the density of reactive sites, the ratio between the site's density on the basal and lateral surfaces and the crystallinity of the sheets [11].

There are two types of charges: i) a permanent negative charge on the tetrahedral surface due to the isomorphous substitution of silicon by lower valence cations. ii) a variable charge which can be either positive or negative according to pH solution and the protonation/deprotonation reaction in the aqueous phase. This variable charge is mainly affected by the silanol (Si-OH) and aluminol (Al-OH) groups on broken edges, and the aluminol (Al-OH) groups on the octahedral surface [9]–[15].

The density of reactive sites of the edge surface is greater than that of alumina and silica faces ; as a consequence, the variation of the zeta potential measured on the slipping plane of the electrical double layer as a function of the pH is mainly due to the variation of the edges charges of the kaolinite platelets [2], [14], [16].

Under temperature, the structure of kaolinite sheets undergoes several important transformations. A first one is due to the dehydroxylation of the kaolinite structure as follows:

$$Al_2O_3.\,2SiO_2.\,2H_2O \xrightarrow{400-700\,^{\circ}C} Al_2O_3.\,2SiO_2 + 2H_2O \quad (1)$$

This transformation is based on the removal of structural water leading to an amorphous phase. This step occurs in stages: starting with the loss of the octahedron chain where the Al changes its coordination from 6 to 4, then that of the tetrahedrons at a higher temperature [14], [17]–[22]. This process is highly dependent on many factors such as kaolinite characteristics (crystallinity,

structure, particle size, and shape, etc.) and many experimental factors such as heating rate and sample processing [23] [17].

A better understanding of the surface properties in aqueous suspension of kaolinite is required in order to modify the platelets reactivity by thermal or chemical pre-treatment (acid washing, organic modification, etc.) [7], [24], [25] to attempt more sophisticated applications [19], [20]. Electrokinetic properties of kaolinite suspensions can be characterized by acoustophoresis. This technique can simultaneously measure the zeta potential and the particle size in colloidal systems without dilution since it involves the measurement of a sound wave generated by the particles rather than devices using optical techniques such as light scattering. Based on the Electrokinetic Sonic Amplitude (ESA) effect, the dynamic mobility is extracted from ESA, the size distribution and the zeta potential are calculated by fitting theory to the dynamic mobility spectra with the ESA or attenuation. By using a wide range of high frequencies for the electroacoustic and ultrasonic attenuation spectrum, the electrokinetic properties of colloids and the interactions between platelets are better characterized (i.e. face/face, edge/edge face/edge). This method allows to compare raw materials with different particle size, it is also possible to eliminate the Smoluchowski approximation which gives an underestimation of the zeta potential because it is calculated from a low frequency mobility magnitude using the thin double layer. Thus, the zeta potential can be used to monitor and control the colloid stability and as an indicator of the particle surface chemistry.

Hence, in this study, two different kaolins very rich in kaolinite are used. They have different characteristics in terms of crystallinity, grain shape, sheet stacking, and basal face/edge ratio. The objective is to characterize the electrokinetic properties of aqueous suspensions of these two kaolins by Acoustophoresis and to emphasize the relationship between the electrokinetic properties of kaolin, the physico-chemical characteristics, and the thermal pre-treatment between 200 and 800 °C. Two specific molecules were also used to characterize the reactivity of the basal and lateral faces according to the pH.

2. Experimental

2.1 Materials

Two commercial kaolins supplied by Imerys company (Limoges, France) were used in this study. K1, a kaolin from Brazil (96 wt% kaolinite) and K2, a kaolin from the USA (93 wt% kaolinite). The chemicals used in this study include: 4,5-Dihydroxy-1,3-benzenedisulfonic acid disodium salt monohydrate (Tiron, $C_6H_4Na_2O_8S_2.H_2O$) and trisodium citrate anhydrous 99% ($C_6H_5Na_3O_7$ 2 H_2O) purchased from ACROS Organics and ThermoFisher (Kandel) GmbH respectively. Hydrochloride acid (HCl, 1N) and sodium hydroxide (NaOH, ≥ 98%) solutions purchased from Sigma-Aldrich were used for pH adjustment.

2.2 Preparation of suspensions

All suspensions for acoustophorometric measurements are prepared with 2 vol% solid content. First, distilled water and dispersant (Tiron/citrate) are mixed, then the kaolin powder is added and the mixture is manually stirred. Hereafter the suspension was submitted to ultrasonic treatment (Vibra-cell 75041, BioBlock Scientific) for 2 min to break particle agglomerates. Finally, the suspension was let for 12 hours on a roller mixer operating before the measurement.

2.3 Techniques of characterization

2.3.1 Chemical and physical analysis

The chemical composition of raw materials was determined thanks to the X-Ray fluorescence (XRF) method using a sequential X-ray fluorescence spectrometer, PANalytical, modèle Zetium. The specific surface area was determined by the BET method Micromeritics 3Flex using nitrogen gas for adsorption. The measurements were carried out after two degassing steps, first at 90 °C for 30 min, followed by a second at 250 °C for 4 h.

2.3.2 X-ray diffraction

The X-Ray diffraction (XRD) pattern of kaolin powders was recorded using a Bruker D8 Advance diffractometer with Cu Kα radiation (λ_{Cu}= 1.54056 Å), at a step scan of 0.02 operated at a voltage of 40 KV with an electric current of 40 mA and over the 2θ range from 5 to 60°.

2.3.3 Scanning electron microscopy

Scanning electron microscopy (SEM) observations were performed using MEB-Env Quanta 450 instrument. The observation was operated at different accelerating voltages (5 to 10 kV). A layer of about 15 nm of Au-Pd was deposited on the sample to ensure suitable electronic conduction at the surface.

2.3.4 Acoustophoresis

Zeta potential measurements were conducted as a function of the pH on the raw materials dispersed at 2.0 vol% in deionized water with an ESA analyzer (AcoustoSizer II S flow through system, Colloidal Dynamics). The apparatus includes sensors for measuring pH, ionic conductivity, and temperature.

The electroacoustic method used in the AcoustoSizer involves the application of an electric field of very high frequency (MHz). This causes the oscillation of the electrically charged colloidal particles in the suspension because of their surface charge and a sound wave of the same frequency is generated. The motion of the particles is then calculated by sound wave analysis which is related to the dynamic mobility. Dynamic mobility is a complex quantity characterized by the magnitude and the phase angle at each frequency. Measurements were performed at thirteen different frequencies (1-20 MHz), with the Enhanced Attenuation Sensor which allows the acoustic pulse to pass only once across the colloid. The advantage of the enhanced attenuation cell is that it can measure much greater attenuations, both because it has a shorter path length and because a much higher voltage is applied across the transducer to generate the driving ultrasonic signal. The set of quantities is called the attenuation spectrum and makes it possible to calculate the size distribution and then the zeta potential by getting the best fit of the spectrum. This theory was initially developed for spherical particles with a low surface conductance but can be applied for platelets if no agglomerates (house of cards) are formed [26]–[28]. Furthermore, measurements take particle size in consideration to calculate zeta potential by getting the best fit of the spectrum, which allows to compare between raw materials with different particle size.

Zeta potential measurements versus pH were made with the automated AcoustoSizer II pH titration system. All experiments were conducted with the pH progressing from basic to acidic solution conditions. Firstly, the pH was fixed at 10 with 1.0 mol/L sodium hydroxide solution, then titrations were carried out by adding 1.0 mol/L hydrochloric acid solution. The following conditions are met:

i) Particle size distribution is constant during the whole experiment in the studied range of pH, which confirms that no agglomerations were formed.

ii) Ionic strength is constant during the titration ($0.5\ 10^{-2}$ and $0.7\ 10^{-2}$ M for K1 and K2 respectively).

iii) The electrolytes concentration is high enough to consider that the contribution of lateral surfaces to the surface charge is not hidden by the basal one [10].

2.3.5 Thermal treatment and analysis of kaolin powders

K1 and K2 samples were placed in a furnace under air and submitted to a thermal treatment with a heating rate of 3 °C.min^{-1} to reach the maximum temperature in the 200 – 800 °C range, followed by a plateau of 5 hours. The heated samples were then characterized by Acoustophoresis following the same procedure as described in 2.2.

Setaram Labsys Evo was used to perform the differential thermal (DT) and thermogravimetric (TG) analyses using the following thermal program: from 30 °C to 1400 °C with heating and cooling rate of 5 °C/min, respectively.

3. Results and discussion

3.1 Mineralogy and chemical composition of the kaolin

The main characteristics of these kaolins are presented in table 1. The ratio of aluminium and silicon (Al/Si) is approximately 1, small quantities of Fe_2O_3 and TiO_2 are detected in the two powders that could be due to substitutions of Al and Si in the layers. Some ppm of alkaline and alkaline earth oxides is also detected.

Table. 1. Chemical and physical characterization of kaolin powders K1 and K2

	K1	K2
Oxide (wt%)		
Al_2O_3	40.36	40.02
SiO_2	43.34	43.44
P_2O_5	0.04	0.30
SO_3	0.04	0.06
K_2O	0.07	0.22
TiO_2	0.52	0.52
Fe_2O_3	0.62	1.00
ZrO_2	0.03	0.00
CaO	0.00	0.32
SrO	0.00	0.02
Loss on ignition (LOI)	15.41	15.08
BET specific area (m^2/g)	6	26

The SEM images of the raw kaolins (Fig. 1) show that the grains of the two kaolin powders have different shapes and sizes. K1 grains are platelet-shaped and almost hexagonal with regular edges, whereas the K2 sample is composed of blocky kaolinite agglomerates, the platelets have an irregular shape and the edges are smooth. The average length of the K1 platelets is in a very large range varying from 0.1 to 3 µm with an average thickness of K1 platelets measured in the 30-35 nm range. The K2 grains have a similar thickness but a smaller range of length (0.1-1 µm). The specific surface area of K2 (26 $m^2. g^{-1}$) is around four times higher than K1 (7 $m^2. g^{-1}$); suggesting that the crystallographic structure of the K2 sample kaolinite should have some defaults [29].

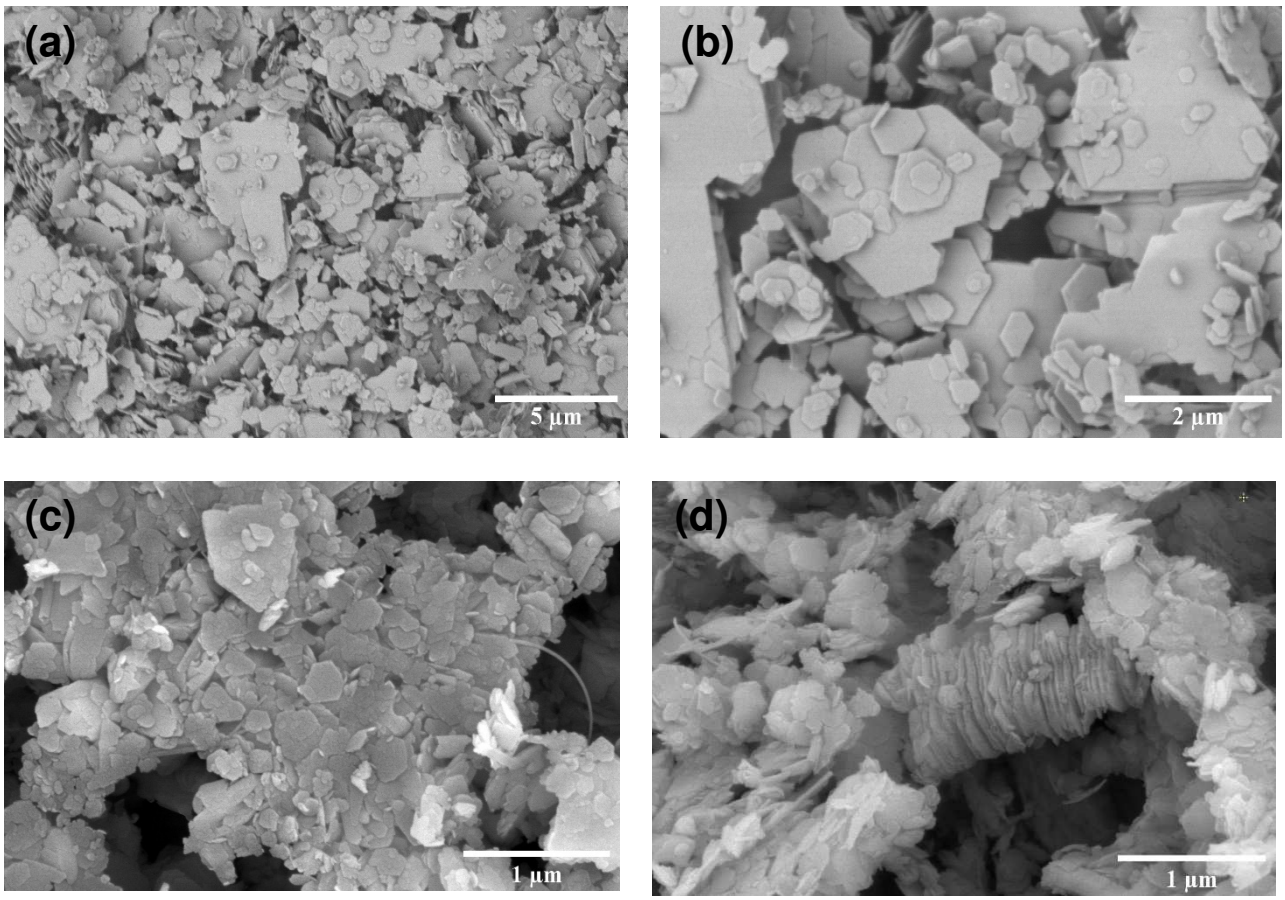

Figure. 1. SEM images of K1 (a) and (b), SEM images of K2 (c) and (d).

3.2 XRD patterns after thermal treatment (200 – 800 °C)

The XRD patterns were carried out on K1 and K2 samples after thermal treatment in the 200 – 800 °C range and are shown in Fig. 2. For the two kaolins, the kaolinite phase remains crystallized until a temperature of 400 °C, well-defined peaks of diffraction are observed. For temperatures greater than 400 °C, kaolinite diffraction peaks are not detected due to the destruction of the crystalline structure caused by the dehydroxylation step. The removal of water leads to a destabilization of the layer stacking and structure, followed by the delamination inside the layer between the silica tetrahedra and the alumina octahedra, the bonds between octahedra and tetrahedra and within the octahedra are broken which influences the structure of the octahedral layer: it finally leads to the change of the coordination of aluminium from 6 to 4 [29], [30]. However, the tetrahedral layer (SiO_4) remains stable during this transformation. The compound becomes amorphous for

temperatures around 600 °C where all the diffraction peaks of kaolinite disappear (zoom on 600 °C et 800 °C (a) in supplementary information). Further increasing the temperature to 800 °C, the diffraction patterns of calcined kaolinite shows no difference from that at 600 °C. Furthermore, quartz peak in the K2 kaolin are always visible during the thermal treatment at different temperatures.

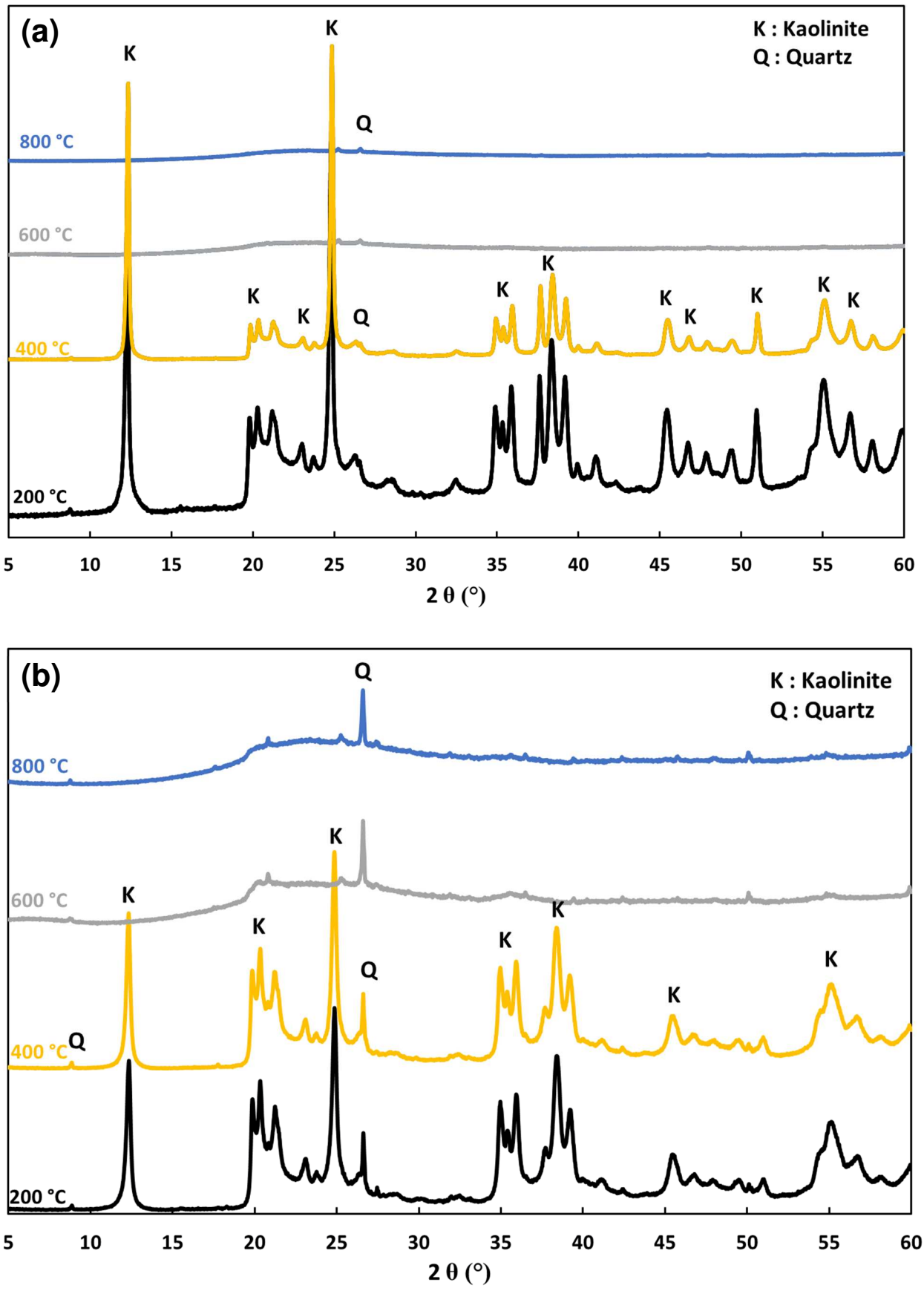

Figure. 2. XRD patterns of kaolin K1 (a) and K2 (b) heat treated at different temperatures

3.3 Zeta potential analysis

3.3.1 Untreated kaolin powder

Fig. 3 shows zeta potentials of both kaolins as a function of pH. Whatever the pH, the electrokinetic properties of these two kaolins are different. The highest potential amplitude (-75 and -55 mV, respectively for K1 and K2) is measured at basic pH 10, the potential amplitude decreases with pH to reach a value of -5 mV at pH 3 for K1, and -10 mV at pH 3.5 for K2. For kaolin K1, the amplitude of the potential remains high until pH 6.5 (-70 mV), then decreases almost linearly to reach nearly 0 mV at pH 3. For kaolin K2, the amplitude decreases progressively from -55 to -40 mV (pH 6) and more rapidly for lower pH but with a lower slope than for K1, the potential is still -10 mV at pH 3.5. Since these kaolins are mostly composed of kaolinite, the measured potential depends on the variations of charges on the surface of the kaolinite platelets.

At pH 10, the faces and edges are negatively charged and the overall potential of the platelets is negative with a strong amplitude. This negative surface charge is due to the ionisation of OH surface groups and to the permanent charge due to cationic substitution in the polyhedral layers. The kaolinite of kaolin K1 contains fewer defects in the structure of platelets and in the stacking assuming that the density of reactive hydroxyl sites should be higher which leads to higher amplitudes and potential variations than for the kaolinite of kaolin K2.

The ionic conductivity is constant for each kaolin suspension during titrations, however, there is a slight difference between both kaolins. We considered that ionic strength is quite similar between the suspensions of the two kaolins and the differences of the zeta potential is mainly due to the surface chemistry.

When the pH decreases, protonation reactions occur around aluminols and silanols sites: the silanols of the edges become neutral and the contribution of the silica face is supposed to remain constant and low over the whole range of pH. Then the negative contribution to the surface charge given by silanol groups decreases. In a first time, the aluminols of the edges and of the alumina basal surface become neutral and positively charged, generating a positive contribution to the surface charge of

the platelets. For these kaolins, that should occur around pH 6.5 where the potential slope changes. This pH is critical for charge state of clay mineral platelets in various studies [10], [11] and could correspond to IEP of edges. At very acidic pH, this positive contribution is nearly equal to the negative one.

A greater amount of atomic stacking defects in the sheets would lead to a lower density of surface hydroxyl groups. It is assumed that the zeta potential of a kaolinite platelet is the resultant of both the contributions of the surface charge of the faces and of the edges. For a higher defect rate, the contributions are lower in intensity and if we consider that the contribution of the faces is constant and negative for the silica face and very little variable for the alumina face, the variation of the potential depends on that of the edges potential. For kaolin K2, the contribution of the edges is not much higher than that of the faces because the kaolinite is less crystallized thus there are less reactive sites and thus the amplitude variations are lower than K1. Several previous studies with acoustophoresis as the main characterization method have been carried out [2], [13], [31], [32] but few of them use the multifrequency option and the analysis of ESA or Attenuation spectra.

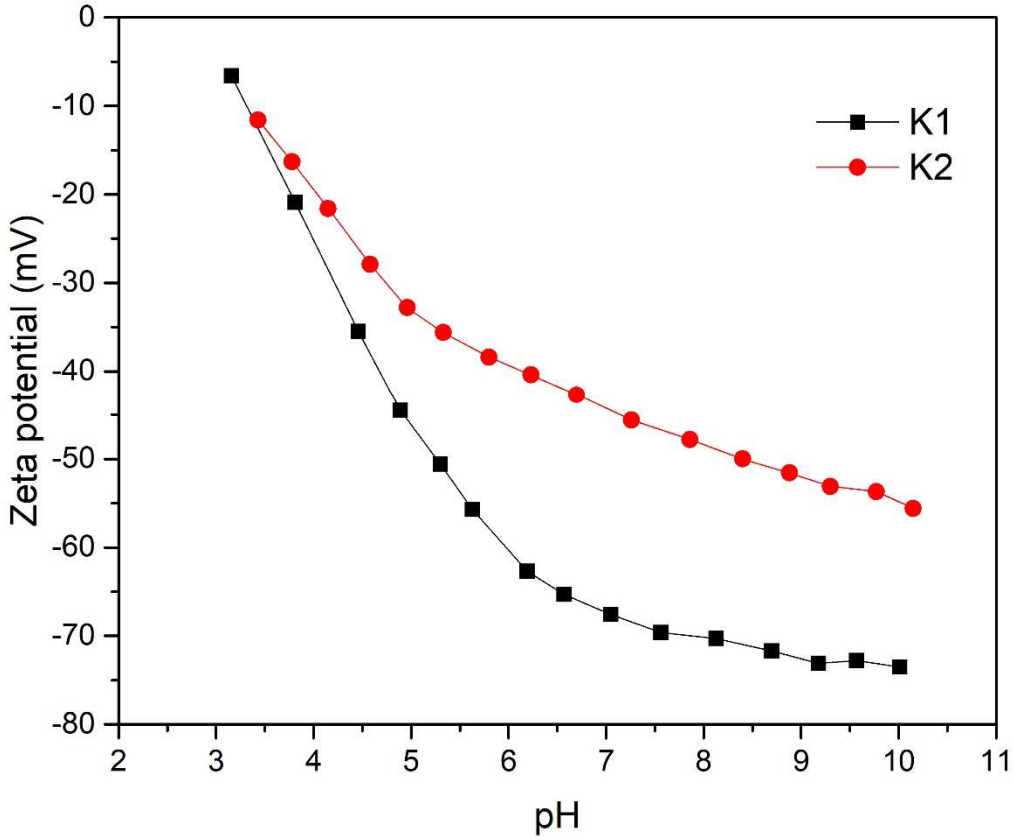

Figure. 3. Zeta potential (mV) of K1 and K2 as a function of pH

3.3.2 Thermal treated kaolin powder

Fig. 4 reports the electrokinetic properties of the two kaolins at different treatment temperatures.

0 < T °C < 200 °C

In this temperature range, the electrokinetic properties of the kaolins vary slightly and are similar to those of the untreated powder. The value of the potential in basic medium is lower by 5 mV when the powder is treated at 200 °C for both kaolins.

200 °C < T °C ≤ 400 °C

After heat treatment at 400 °C, the electrokinetic properties of both kaolins vary considerably. For kaolin K1, the potential in basic medium is the same up to pH 8; for pH < 8, it decreases with a steep slope to become positive from pH 4.5 and reaches the value of +12 mV at pH 3.5. For kaolin

K2, the measured potential is much lower whatever the pH, it varies between -15 mV and +5 mV and becomes positive for pH 4.5.

Treatment at 400 °C increases the positive contribution to the zeta potential. The evolution of the permanent negative charge as a function of temperature should remain low or even decreases with the destruction of the polyhedral. Even if the kaolinite of K1 and K2 keeps its initial state of crystallinity according to the XRD (Fig. 2), the surface properties of the platelets in water are significantly modified. The positive contribution to the zeta potential increases. For K1, the zeta amplitude is very high, thus, there are a lot of reactive sites with either an increase of Al-OH sites or a decrease in Si-OH sites. However, for K2, the zeta amplitude decreases sharply; there are less reactive sites than K1 which confirms that the rate of atomic stacking defects is higher for kaolin K2 and the dehydroxylation occurs earlier in temperature (see DTA in supplementary information).

T °C ≥ 600 °C

For K2, the positive contribution decreases with increasing the temperature and the potential remains negative over the whole pH range for a thermal treatment at 800 °C. The same phenomenon is observed for K1 with higher potential values and variations due to its higher crystallinity, even though from 600 °C, the kaolinite of both kaolins is amorphous (see XRD in Fig. 4).

This study is thus very original, while using electrokinetic properties as a function of temperature treatment of kaolin powders to show the increase in atomic stacking defects during the dehydroxylation process that occurs at lower temperatures for K2. It also shows an increase in the positive contribution of the zeta potential compared to the negative one up to 400 °C for K1 and K2 and a decrease in this contribution for higher temperatures. This increase in positive contribution may be due to the proton delocalization and predehydroxylation of kaolinite [13], [33].

The evolution of kaolinite structure in temperature has been studied by NMR in many studies [21], [30], [34]. Based on a study reported by Han [29] to analyse the changes in crystal structure during dehydroxylation of kaolinite, NMR measurements have been performed on kaolinite samples

soaked with D_2O during heating. At room temperature, all OH groups could be exchanged by OD groups. According to their results, D_2O adsorbs in the inner-surface of the kaolinite. These authors show that in the temperature range of 100-300 °C, two layers of kaolinite slip away from each other, promoting a transformation of the inner surface OH/OD groups into outer OH/OD groups and the release of intercalation water. Thus, the number of Al-OH sites increases during water-removal. As the temperature increases, OD groups disappear until complete disappearance at 650 °C.

Kaolinite still has the same crystallinity in both kaolins until 400 °C (see XRD in Fig. 4), but the electrokinetic properties are different as a function of temperature. For K2, variations of the zeta potential are observed from 200 °C due to the presence of defects. Between the two kaolins, there is always the same tendency but the temperatures are not the same. At 400 °C, the potential becomes positive at pH 4, the positive contribution of Al-OH sites (face or edge) is more important, and as a consequence, the defects in sheet stacking should lead to a higher Al-OH/Si-OH ratio than at 200 °C and without heat treatment. At pH 10, all OH sites are negative, so the decrease in potential values with treatment temperature is due to the decrease of the density of reactive hydroxyl sites with temperature, assuming that this is related to the loss of crystallinity and the increase in defects (see XRD in Fig. 2).

At pH 3.5, the potential becomes less negative, then positive at 400 °C, the values are always lower in absolute value with K2. At higher temperatures, the positive contribution continues to decrease in both kaolins indicating a decrease in the positive contribution (Al-OH sites). According to Hann [29], the slipping of the sheet should lead to a higher alumina basal surface exposed (Fig. 5).

In comparison with XRD and DTA/GTA (supplementary information), changes in the electrokinetic properties of the powders occur at temperatures lower than the temperatures at which the dehydroxylation can be observed. Hence, Zeta potential measurements by acoustophoresis technique allow to detect changes in the surface chemistry properties of kaolinite aqueous suspensions related to the modification of the atomic stacking and the increase of stacking defects at temperatures lower than 400 °C. It also allows to determine the contribution of the Al-OH sites by

examining the properties in acidic medium (pH < 6.5). Since the protonation of Al-OH sites to Al-OH^{2+} occurs in acidic media, it is necessary to perform the measurements in this pH range to detect the differences.

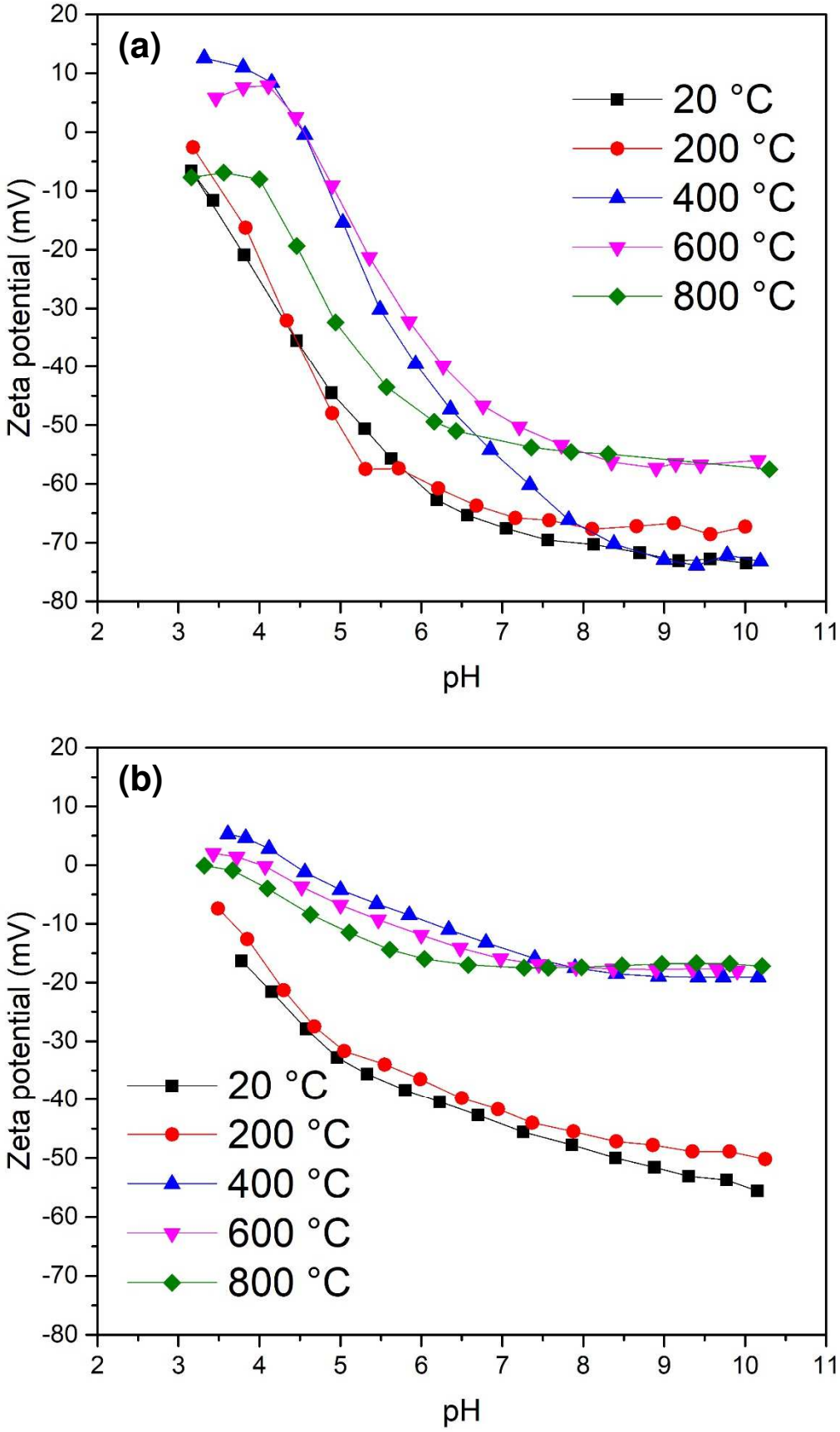

Figure. 4. Zeta potential for K1 (a) and K2 (b) kaolins heat treated at different temperature as a function of pH

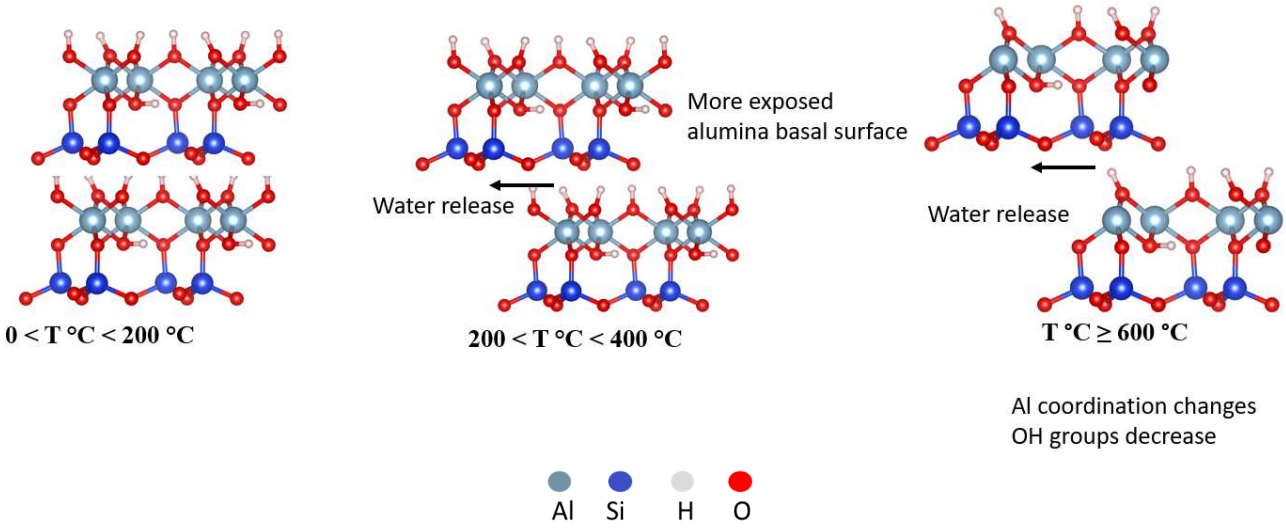

Figure. 5. Kaolinite structure modification under thermal treatment

3.4 Study of the dispersant adsorption on kaolinite

3.4.1 Untreated kaolin powder

Tiron and citrate have two different chemical structures and different adsorption on kaolinite. Citrate is a highly charged small anion commonly used with kaolinite thanks to its high surface affinity at the solid/water interface [13], [35]. The molecule of Tiron complexes several cations (Al^{3+}, Ti^{4+}, Zr^{4+}, Fe^{3+} etc…) in aqueous suspensions and it adsorbs onto the corresponding oxide surfaces. It is a derivative of catechol with two sulfonate groups, its use with kaolinite has not been mentioned in the literature [36]–[38],

Fig. 6 shows that the addition of Tiron or citrate does not modify the electrokinetic properties of both kaolins in basic medium. The electrostatic interactions between the platelets and the anions are not favourable to their adsorption and their contribution to the surface charge is negligible. It is from pH 7 that the interactions with molecules become favourable, consequently, their adsorption increases the negative contribution to the zeta potential. At pH 3, the maximum contribution is measured in acidic medium.

Moreover, the ionization of the molecule influences the surface chemistry of the kaolinite. Tiron is an anion whatever the pH. However, citrate is neutralized when the pH decreases. Without

molecules, Al-OH sites become $AlOH^{2+}$ which makes a positive contribution to the surface charge. When molecules are added, the -OH group is replaced by Tiron or citrate. This adsorption on Al-OH sites which normally protonate leads to a decrease in the positive contribution of surface charge.

The addition of these molecules modifies the electrokinetic properties of kaolin K1, especially from pH 6.5. With 1 wt% citrate, at pH 3, the potential is measured at -40 mV instead of 0 without molecules for K1. The potential difference with citrate is much higher than with Tiron even if more Tiron is added.

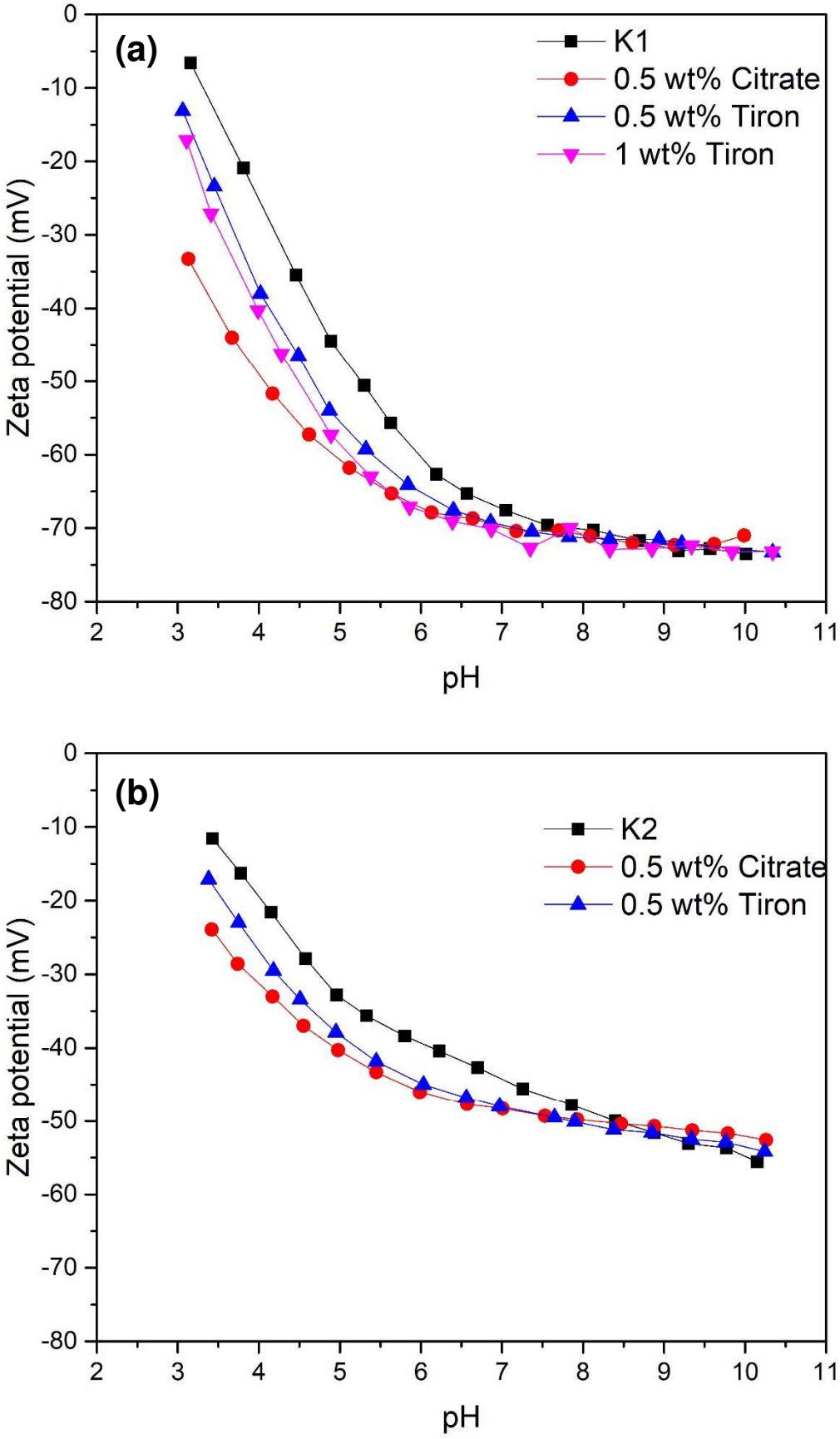

Figure. 6. Zeta potential (mV) of K1 (a) and K2 (b) with different additions as a function of pH

Fig. 7 shows the adsorption of these two molecules on kaolinite according to two hypotheses:

i) Citrate molecules should adsorb onto alumina surfaces but predominantly on the edge sites of the platelet of kaolinite [38] which represent the major contribution of the global surface charge as mentioned previously due to the high reactive sites.

ii) Tiron molecules should adsorb on the alumina basal surface of kaolinite thanks to the presence of two hydroxyl groups derived from catechol [39]. The distance between two OH catechol groups corresponds to that of two oxygens in the octahedral layer, which favours this adsorption. Therefore, Tiron adsorption on the basal alumina face contributes slightly to zeta potential

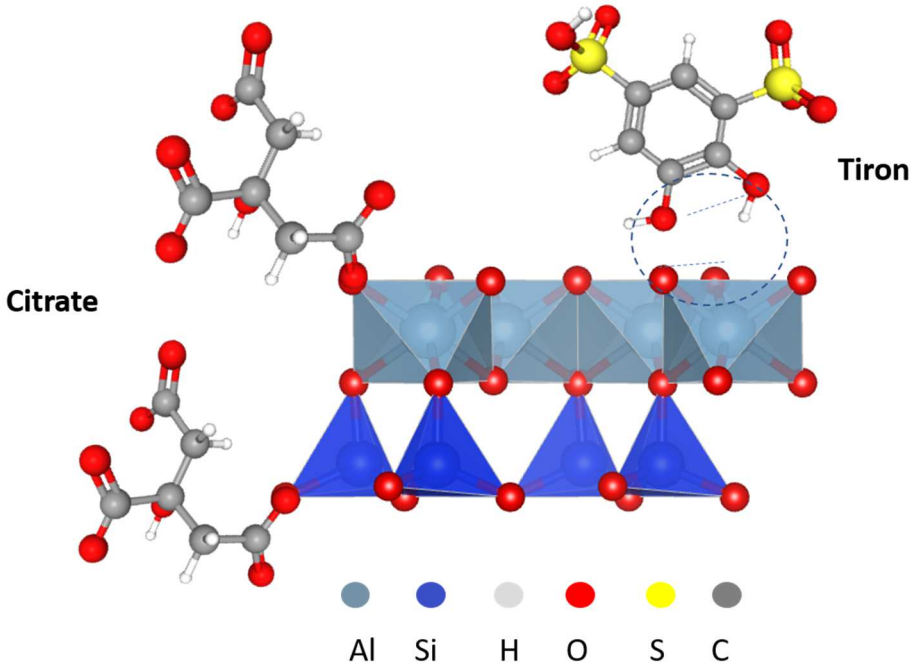

Figure. 7. Molecules specific adsorption on kaolinite in aqueous medium

amplitude (less reactive sites).

3.4.2 Thermal treated kaolin powder

The effect of Tiron on the electrokinetic properties was also studied after thermal treatment of K1 in Fig. 8. At 400 °C, Tiron adsorbs also in neutral medium 6 < pH < 8 and increases the potential by 20 mV. At 600 °C, Tiron adsorbs over the whole pH range and still has the same effect as the 400

°C treated powder indicating the high density of Al-OH sites on basal surface according to the previous hypothesis, even if the kaolinite is amorphous at this temperature. When the powder is treated at 800 °C, the curves are quite similar in basic medium, the potential increases slightly in acidic medium by almost 10 mV. The molecule does not adsorb a lot showing that the kaolinite surface is mainly populated by Si-OH sites. If Tiron molecules adsorb only on the alumina basal face, the 400 °C and 600 °C treatment increases the accessible surface of the alumina faces because of water-removal during the dehydroxylation process which confirms the previous results.

The adsorption of citrate was only studied for 400 °C treated K1 (Fig. 9). The contribution of citrate increases the potential by -20 mV at pH 6 with a maximum of -58 mV around pH 5. It seems that there are many more adsorption sites available with heat treatment even on the edges because of beneficial electrostatic attractions of Al-OH_2^+.

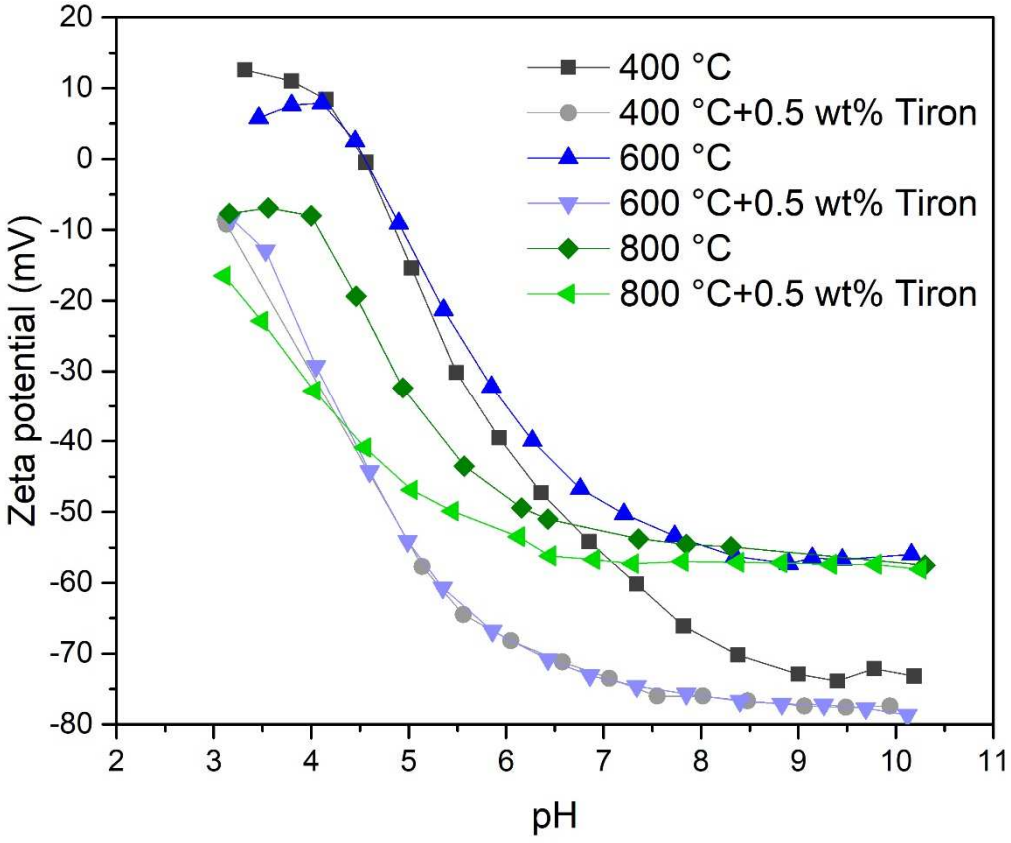

Figure. 8. Zeta potential of thermal treated kaolin K1 with the addition of Tiron

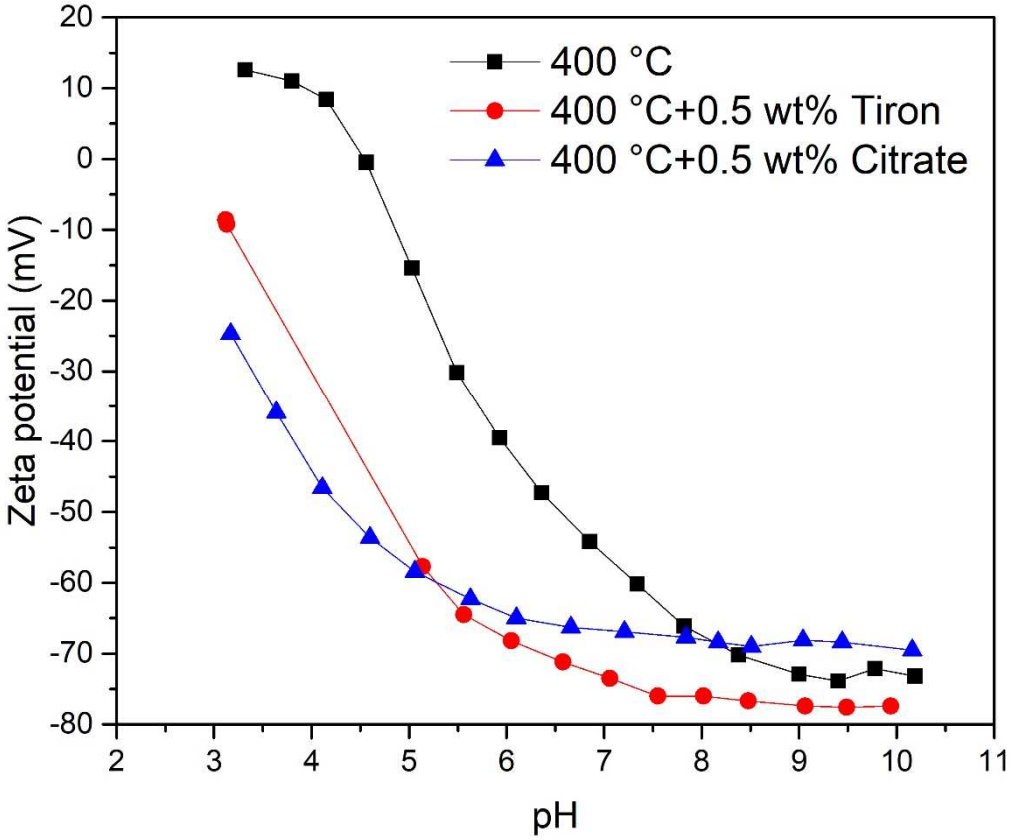

Figure. 9. Zeta potential of thermal treated kaolin K1 at 400 °C with the addition of citrate

4 Conclusion

This research work carried out on the study of the electrokinetic properties of aqueous suspensions of kaolinite highlights:

- The interest of the acoustophoresis technique used which measures the amplitude and the phase shift of the acoustic wave according to a wide frequency range without suspension dilution. This technique allows to study the behaviour of different grain populations of a powder according to their size and therefore to evaluate their state of dispersion. It also

allows to compare the surface chemistry of two powders of the same material but with different particle size distributions.

- The influence of the crystallinity of kaolinite platelets on their surface chemistry in aqueous suspension. The density of surface hydroxyl groups is higher when the stacking defaults of the atoms in the polyhedral layers are lower. Therefore, the amplitude of the measured zeta potential is greater.

- The possibility of differentiating the faces and edges contributions to the zeta potential of the platelets by studying the electrokinetic properties as a function of the pH but also by specifically adsorbing molecules either on the alumina faces (Tiron and citrate) or on the edges (citrate). It has been confirmed that the contribution of the edges is preponderant on the zeta potential variation of the platelets.

- The variation of platelet surface chemistry properties during the amorphous phase formation process after temperature treatment of kaolin powder. The electrokinetic properties of kaolin suspensions treated between 200 and 800 °C successively show an increase in the positive contribution to the zeta potential up to 400 °C for the best-crystallized kaolinite and a decrease in the density of surface hydroxyl groups when the sheets delaminate from 400 °C for the less-crystallized kaolinite. The adsorption of specific molecules such as Tiron on temperature pre-treated kaolinite platelets confirms an increase in the density of aluminol sites compared to silanols.

The kaolinite properties have been mainly studied, in powder form, at temperatures higher than 500 °C after the dehydroxylation step with the following characterization techniques; XRD, DTA, FTIR, RMN) [24], [30], [40], [41]. This work, conducted with aqueous suspensions, shows that the zeta potential of kaolinite platelets completes the characterization of their surface properties in the 200 – 800 °C range.

As kaolin is a raw material for ceramic shaping, this work makes it possible to control the dispersion and the reactivity of kaolinite in a mixed system (i.e. with alumina) and then the crystallization of the mullite according to the starting formulation (crystallinity state, pre-treatment, addition of molecules, etc…), presenting a variety of physico-chemical properties converging towards a wide range of applications.

Acknowledgements: The authors are grateful to the Région Nouvelle Aquitaine for the financial support of this research work

5. References

[1] B. Bauluz, « HALLOYSITE AND KAOLINITE: TWO CLAY MINERALS WITH GEOLOGICAL AND TECHNOLOGICAL IMPORTANCE », *Revista de la Real Academia de Ciencias. Zaragoza.*, vol. 70, p. 1-33, janv. 2015.

[2] X. Zhu, Z. Zhu, X. Lei, et C. Yan, « Defects in structure as the sources of the surface charges of kaolinite », *Applied Clay Science*, vol. 124-125, p. 127-136, mai 2016, doi: 10.1016/j.clay.2016.01.033.

[3] M. E. Awad, A. López-Galindo, M. Setti, M. M. El-Rahmany, et C. V. Iborra, « Kaolinite in pharmaceutics and biomedicine », *International Journal of Pharmaceutics*, vol. 533, n° 1, p. 34-48, nov. 2017, doi: 10.1016/j.ijpharm.2017.09.056.

[4] R. j. King, « Kaolinite », *Geology Today*, vol. 25, n° 2, p. 75-78, 2009, doi: 10.1111/j.1365-2451.2009.00711.x.

[5] P. Alaba, Y. M. Sani, et W. Daud, « Kaolinite properties and advances for solid acid and basic catalyst synthesis », *RSC Advances*, vol. 5, p. 101127-101147, nov. 2015, doi: 10.1039/C5RA18884A.

[6] X. Liu, Z. Chen, Z. Chen, M. Megharaj, et R. Naidu, « Remediation of Direct Black G in wastewater using kaolin-supported bimetallic Fe/Ni nanoparticles », *Chemical Engineering Journal*, vol. 223, p. 764-771, mai 2013, doi: 10.1016/j.cej.2013.03.002.

[7] « Removal of heavy metals and dyes by clay-based adsorbents: From natural clays to 1D and 2D nano-composites - ScienceDirect ». https://www.sciencedirect.com/science/article/pii/S1385894720336962 (consulté le 28 avril 2022).

[8] M. Jiang, X. Jin, X.-Q. Lu, et Z. Chen, « Adsorption of Pb(II), Cd(II), Ni(II) and Cu(II) onto natural kaolinite clay », *Desalination*, vol. 252, n° 1, p. 33-39, mars 2010, doi: 10.1016/j.desal.2009.11.005.

[9] P. Hu et H. Yang, « Insight into the physicochemical aspects of kaolins with different morphologies », *Applied Clay Science*, vol. 74, p. 58-65, avr. 2013, doi: 10.1016/j.clay.2012.10.003.

[10] E. Tombácz et M. Szekeres, « Surface charge heterogeneity of kaolinite in aqueous suspension in comparison with montmorillonite », 2006, doi: 10.1016/J.CLAY.2006.05.009.

[11] E. Tombácz et M. Szekeres, « Colloidal behavior of aqueous montmorillonite suspensions: the specific role of pH in the presence of indifferent electrolytes », *Applied Clay Science*, vol. 27, n° 1, p. 75-94, oct. 2004, doi: 10.1016/j.clay.2004.01.001.

[12] M. Alkan, Ö. Demirbaş, et M. Doğan, « Electrokinetic properties of kaolinite in mono- and multivalent electrolyte solutions », *Microporous and Mesoporous Materials*, vol. 83, nº 1, p. 51-59, sept. 2005, doi: 10.1016/j.micromeso.2005.03.011.
[13] E.-J. Teh, Y. K. Leong, Y. Liu, A. B. Fourie, et M. Fahey, « Differences in the rheology and surface chemistry of kaolin clay slurries: The source of the variations », *Chemical Engineering Science*, vol. 64, nº 17, p. 3817-3825, sept. 2009, doi: 10.1016/j.ces.2009.05.015.
[14] V. Gupta, M. A. Hampton, J. R. Stokes, A. V. Nguyen, et J. D. Miller, « Particle interactions in kaolinite suspensions and corresponding aggregate structures », *Journal of Colloid and Interface Science*, vol. 359, nº 1, p. 95-103, juill. 2011, doi: 10.1016/j.jcis.2011.03.043.
[15] Y.-H. Wang et W. Siu, « Structure characteristics and mechanical properties of kaolinite soils. I. Surface charges and structural characterizations », *Canadian Geotechnical Journal*, vol. 43, p. 587-600, janv. 2011, doi: 10.1139/t06-026.
[16] H. Wang, C. Li, Z. Peng, et S. Zhang, « Characterization and thermal behavior of kaolin », *Journal of Thermal Analysis and Calorimetry*, vol. 105, juill. 2011, doi: 10.1007/s10973-011-1385-0.
[17] P. Ptáček, F. Frajkorová, F. Šoukal, et T. Opravil, « Kinetics and mechanism of three stages of thermal transformation of kaolinite to metakaolinite », *Powder Technology*, vol. 264, p. 439-445, sept. 2014, doi: 10.1016/j.powtec.2014.05.047.
[18] K. Heide et M. Földvari, « High temperature mass spectrometric gas-release studies of kaolinite Al2[Si2O5(OH)4] decomposition », *Thermochimica Acta*, vol. 446, nº 1, p. 106-112, juill. 2006, doi: 10.1016/j.tca.2006.05.011.
[19] R.-P. Chen, X.-Y. Liu, W. Yang, Z. Xia, X. Kang, et A. Lushnikova, « Wetting behavior of metakaolinite on the basal surfaces – Molecular dynamics study », *Computers and Geotechnics*, vol. 129, p. 103863, janv. 2021, doi: 10.1016/j.compgeo.2020.103863.
[20] E. Horvath, R. Frost, E. Mako, J. Kristóf, et T. Cseh, « Thermal treatment of mechanochemically activated kaolinite », *Thermochimica Acta*, vol. 404, p. 227-234, sept. 2003, doi: 10.1016/S0040-6031(03)00184-9.
[21] J. Cheng *et al.*, « Dehydroxylation and Structural Distortion of Kaolinite as a High-Temperature Sorbent in the Furnace », *Minerals*, vol. 9, p. 587, sept. 2019, doi: 10.3390/min9100587.
[22] H. Cheng, Q. Liu, J. Yang, S. Ma, et R. L. Frost, « The thermal behavior of kaolinite intercalation complexes-A review », *Thermochimica Acta*, vol. 545, p. 1-13, oct. 2012, doi: 10.1016/j.tca.2012.04.005.
[23] P. Ptáček, D. Kubátová, J. Havlica, J. Brandštetr, F. Šoukal, et T. Opravil, « The non-isothermal kinetic analysis of the thermal decomposition of kaolinite by thermogravimetric analysis », *Powder Technology*, vol. 204, nº 2, p. 222-227, déc. 2010, doi: 10.1016/j.powtec.2010.08.004.
[24] C. Zhang, Z. Zhang, Y. Tan, et M. Zhong, « The effect of citric acid on the kaolin activation and mullite formation », *Ceramics International*, vol. 43, nº 1, Part B, p. 1466-1471, janv. 2017, doi: 10.1016/j.ceramint.2016.10.115.
[25] E. Aguiar *et al.*, « materials Acetylation of Eugenol over 12-Molybdophosphoric Acid Anchored in Mesoporous Silicate Support Synthesized from Flint Kaolin », *Materials*, sept. 2019, doi: 10.3390/ma12182995.
[26] M. Loewenberg et R. W. Ob́rien, « The dynamic mobility of nonspherical particles », *Journal of Colloid and Interface Science*, vol. 150, nº 1, p. 158-168, avr. 1992, doi: 10.1016/0021-9797(92)90276-R.
[27] R. W. O'Brien, D. W. Cannon, et W. N. Rowlands, « Electroacoustic Determination of Particle Size and Zeta Potential », *Journal of Colloid and Interface Science*, vol. 173, nº 2, p. 406-418, août 1995, doi: 10.1006/jcis.1995.1341.

[28] R. J. Hunter, « Recent developments in the electroacoustic characterisation of colloidal suspensions and emulsions », *Colloids and Surfaces A: Physicochemical and Engineering Aspects*, vol. 141, n° 1, p. 37-66, oct. 1998, doi: 10.1016/S0927-7757(98)00202-7.
[29] Y. Han, Z. Yan, L. Jin, J. Liao, et G. Feng, « In situ study on interactions between hydroxyl groups in kaolinite and re-adsorption water », *RSC Adv.*, vol. 10, n° 29, p. 16949-16958, avr. 2020, doi: 10.1039/D0RA01905D.
[30] K. Yan, Y. Guo, L. Fang, L. Cui, F. Cheng, et T. Li, « Decomposition and phase transformation mechanism of kaolinite calcined with sodium carbonate », *Applied Clay Science*, vol. 147, p. 90-96, oct. 2017, doi: 10.1016/j.clay.2017.07.010.
[31] S. B. Johnson, A. S. Russell, et P. J. Scales, « Volume fraction effects in shear rheology and electroacoustic studies of concentrated alumina and kaolin suspensions », *Colloids and Surfaces A: Physicochemical and Engineering Aspects*, vol. 141, n° 1, p. 119-130, oct. 1998, doi: 10.1016/S0927-7757(98)00208-8.
[32] P.-I. Au et Y.-K. Leong, « Rheological and zeta potential behaviour of kaolin and bentonite composite slurries », *Colloids and Surfaces A: Physicochemical and Engineering Aspects*, vol. 436, p. 530-541, sept. 2013, doi: 10.1016/j.colsurfa.2013.06.039.
[33] Y. Hu et X. Liu, « Chemical composition and surface property of kaolins », *Minerals Engineering*, vol. 16, n° 11, Supplement 1, p. 1279-1284, nov. 2003, doi: 10.1016/j.mineng.2003.07.006.
[34] X. Lin, K. Ideta, J. Miyawaki, Y. Wang, I. Mochida, et S.-H. Yoon, « MAS, STMAS and DQMAS NMR Studies of the Thermal Transformation of Kaolinite », *Appl Magn Reson*, vol. 44, n° 9, p. 1081-1094, sept. 2013, doi: 10.1007/s00723-013-0466-6.
[35] Y.-K. Leong *et al.*, « Controlling attractive interparticle forces via small anionic and cationic additives in kaolin clay slurries », *Chemical Engineering Research and Design*, vol. 90, n° 5, p. 658-666, mai 2012, doi: 10.1016/j.cherd.2011.09.002.
[36] C. Pagnoux, T. Chartier, M. de F. Granja, F. Doreau, J. M. Ferreira, et J. F. Baumard, « Aqueous suspensions for tape-casting based on acrylic binders », *Journal of the European Ceramic Society*, vol. 18, n° 3, p. 241-247, janv. 1998, doi: 10.1016/S0955-2219(97)00115-5.
[37] R. Laucournet, C. Pagnoux, T. Chartier, et J. F. Baumard, « Catechol derivatives and anion adsorption onto alumina surfaces in aqueous media: influence on the electrokinetic properties », *Journal of the European Ceramic Society*, vol. 21, n° 7, p. 869-878, juill. 2001, doi: 10.1016/S0955-2219(00)00287-9.
[38] S.-M. Lin *et al.*, « The synergistic mechanisms of citric acid and oxalic acid on the rapid dissolution of kaolinite », *Applied Clay Science*, vol. 196, p. 105756, oct. 2020, doi: 10.1016/j.clay.2020.105756.
[39] B. Diar-Bakerly, D. Hirsemann, H. Kalo, R. Schobert, et J. Breu, « Modification of kaolinite by Grafting of siderophilic ligands to the external octahedral surface », *Applied Clay Science*, vol. 90, p. 67-72, mars 2014, doi: 10.1016/j.clay.2013.12.020.
[40] I. Daou, G. L. Lecomte-Nana, N. Tessier-Doyen, C. Peyratout, M. Gonon, et R. Guinebretiere, « Probing the Dehydroxylation of Kaolinite and Halloysite by In Situ High Temperature X-ray Diffraction », *Minerals*, vol. 10, n° 5, p. 480, mai 2020, doi: 10.3390/min10050480.
[41] H. He, J. Guo, J. Zhu, P. Yuan, et C. Hu, « 29Si and 27Al MAS NMR spectra of mullites from different kaolinites », *Spectrochimica Acta Part A: Molecular and Biomolecular Spectroscopy*, vol. 60, n° 5, p. 1061-1064, avr. 2004, doi: 10.1016/S1386-1425(03)00337-8.